Quantifying 450 years of limestone weathering induced by salt crystallization on fortifications in Malta and Gozo

Erwan Roussel, Franck Vautier, Olivier Voldoire, Marie-Françoise André, Joann Cassar, Gilles Fronteau, Bruno Phalip, Céline Thomachot-Schneider, Jean-Pierre Toumazet

Quantifying 450 years of limestone weathering induced by salt crystallization on fortifications in Malta and Gozo

ROUSSEL Erwan[1], VAUTIER Franck[2], VOLDOIRE Olivier[1], ANDRÉ Marie-Françoise[1], CASSAR JoAnn[3], FRONTEAU Gilles[4], PHALIP Bruno[5], THOMACHOT-SCHNEIDER Céline[4], TOUMAZET Jean-Pierre[1]

[1] Université Clermont Auvergne, CNRS, GEOLAB, F-63000 Clermont-Ferrand, France

[2] Université Clermont Auvergne, CNRS, Maison des Sciences de l'Homme, F-63000 Clermont-Ferrand, France

[3] University of Malta, Department of Conservation and Built Heritage, Faculty for the Built Environment, Msida MSD 2080, Malta

[4] Université de Reims Champagne-Ardenne, GEGENAA, F-51100 Reims, France

[5] Université Clermont Auvergne, CHEC, F-63000 Clermont-Ferrand, France

Highlights

- SfM photogrammetry and on-site tests were carried out on Maltese fortifications.
- A two-rate weathering regime was highlighted within the building limestones.
- Cohesiveness and water uptake capacity were identified as controlling factors.
- There is no straightforward correlation between durability and surface hardness.

Abstract

Structure from Motion (SfM) photogrammetry, on-site hardness and water absorption tests, and petrographical and porosimetric analyses on targeted samples were carried out on representative areas within six different locations of Maltese fortifications affected by salt weathering. The objective was to quantify the limestone loss over the last half-millennium and to attempt to identify the controlling factors of durability. The results highlight the existence of a two-rate weathering regime within the Miocene Globigerina Limestone which is the main building stone of the Maltese Islands. With a median stone recession of 1.4 mm/century, the subtype locally called *Franka* has resisted atmospheric aggression on average 36 times better than the *Soll* subtype (median stone recession of 50 mm/century). The Oligo-Miocene Coralline Limestone has also resisted well, with a stone recession of on average 1.3 mm/century. Two main controls of the varying durability of these limestones have been identified. First, the water uptake capacity of the least durable, already weathered limestone (*Soll*) is two to three times higher than that of the weathered but more resistant *Franka* and Coralline Limestone (6.3 $g.m^{-2}.s^{-1}$ against 2.5 $g.m^{-2}.s^{-1}$). Second, there is a marked difference in cohesiveness between these limestones. Whereas the weathered, susceptible *Soll* facies is poorly-cemented or microcracked, the exposed durable *Franka* displays an abundant micritic and microsparitic matrix. The statistical relationship between durability and surface hardness is not straightforward, and other controls such as the clay content of limestones should be explored. Investigating a larger number of sites would allow the refining of the limestone durability scale inferred from the present study.

Keywords

Salt weathering

Limestone weathering rates

Maltese Islands

Mediterranean fortifications

1. Introduction

Limestone has been widely used as building stone over the millennia, and the complexity of decay patterns in this rock material subject both to chemical and mechanical weathering has been thoroughly studied (see an overview in Smith et al., 2010). Regarding quantitative studies, a large number of long-term weathering rate studies are available for carbonate stones used in continental and urban monuments, including tombstones (from Geikie 1880 to Meierding 1993). However little is known about historical weathering rates in coastal areas, except for marble (e.g. Cooke et al., 1995; Inkpen and Jackson, 2000), which are metamorphosed carbonate rocks that behave quite differently from sedimentary limestones which are the focus of this paper. To date, only three studies provide historical weathering rates for coastal limestone monuments (Viles and Goudie, 1992; Augeyre 2006, 2008; Gruson, 2013) and they are all restricted to the European Atlantic coast (Table 1). At these sites in S England and SW France, most available recession rates range on average from 1 to 3 mm per century, except for micritic and platy limestones which display much faster recession rates (from 5 to 28 mm per century) than sparitic limestones.

As far as can be ascertained, no quantitative data has been published to date for coastal historical monuments of the Mediterranean Basin, where extensive outcrops of Oligo-Miocene soft and highly porous limestones, easy to carve, have been quarried for millennia

and widely used for building and decoration. It is especially the case in the Maltese Islands which display a rich architectural heritage, including prehistoric temples, Baroque palaces and defensive structures, of which several are inscribed by UNESCO as World Heritage Sites. Most monuments are built in Oligo-Miocene Globigerina Limestone which has been recognized in 2019 by the International Union of Geological Sciences (IUGS) as a Global Heritage Stone Resource, following a proposal submitted by the Faculty for the Built Environment and the Department of Geosciences of the University of Malta (Cassar et al., 2017).

The Globigerina Limestone dates back to the early to mid-Miocene (Aquitanian to Langhian stages, 23–14 Ma**)** and is 20 to 200 m thick (Pedley, 1976, see also the geological map available at continentalshelf.gov.mt). It has been extensively studied over the last decades (e.g. Cassar, 2002, 2004, 2010; Fitzner et al., 1996; Gatt, 2006; Rothert et al., 2007; Vannucci et al., 1994; Zammit and Cassar, 2017). It is a honey-coloured, fine-grained and soft biomicritic limestone, containing > 92% calcite and small amounts of clay minerals, and often displaying bioturbation features (Gatt, 2006). This rapidly absorbing stone has a high porosity, ranging from 24 to 41% (Cassar et al., 2017). In the Maltese salt-laden marine environment (Torfs et al., 1996), many monuments built in Globigerina Limestone have been subject to deterioration and often display conspicuous forms of alveolar weathering (or honeycomb weathering) such as those present on the severely decayed statues of St. Margaret Church at Sannat, on the Island of Gozo (Fig. 1). Alveolar weathering due to salt crystallization is a leitmotiv in the Maltese landscape, and its development has been suggested by Vannucci et al. (1994), Fitzner et al. (1996) and Rothert et al. (2007) to follow a five-stage sequence, from sound stone to totally back-weathered stone, as illustrated in Fig. 2. Gatt (2006) has also proposed a model linking the level of heterogeneity of the Globigerina Limestone to the mode of salt weathering. The

96 severity of weathering damage at some Maltese sites has motivated in the last decades both
97 protective measures such as the installation of polytetrafluoroethylene (PTFE) membranes
98 supported by steel arches anchored by cables over some Megalithic Temples (Cassar et al.,
99 2011, 2018) and extensive restorations of fortifications and historical buildings (Spiteri, 2011).
100
101 Although usually visually homogeneous when freshly cut, the Globigerina Limestone displays
102 two facies, that should be considered as the end members of a variety of subtypes (Diana et
103 al., 2014). These two subtypes can be differentiated on abandoned quarry faces, as recognized
104 for centuries by quarry workers and stonemasons, where a resistant facies traditionally called
105 *Franka* hardens when exposed to the air whereas a less resistant facies traditionally called *Soll*
106 rapidly powders away. They can also be distinguished through salt weathering tests (Fitzner
107 et al., 1996; Rothert et al., 2007; Cassar et al., 2008). Laboratory analyses indicate that the
108 phyllosilicate content of *Soll* is up to four times higher than the one of *Franka* (12% against 3%
109 according to Cassar 1999). Moreover, Cassar (2002) and Rothert et al. (2007) have shown that
110 *Franka* displays larger pores than *Soll* (67% >1µm and 33% <1µm for *Franka* against 42% >1µm
111 and 58% <1µm for *Soll*). And recent analyses performed by Zammit and Cassar (2017) have
112 confirmed that the resistant facies (*Franka*) is characterised by a higher macroporosity and a
113 less abundant insoluble residue than *Soll*.
114
115 As an additional building stone, Coralline Limestone is less abundant in outcrop in the Maltese
116 Islands than the Globigerina Limestone (Fig. 3). The Lower Coralline limestone dates back to
117 the Upper Oligocene (Chattian stage, 28-23 Ma) and is up to 140 m thick, whereas the Upper
118 Coralline limestone dates back to the Upper Miocene (Messinian stage, 7-5 Ma) and is up to
119 160 m thick (Pedley, 1976, see also the geological map available at continentalshelf.gov.mt). The

Coralline limestone has been empirically recognized for millennia as a resistant building stone. For this reason, it has been used to build the external walls of the Mnajdra and most of Ġgantija prehistoric temples as well as some of the fortifications of of the Gozo Citadel (Cassar, 2002), and the lower courses of ramparts (Spiteri 2008). The porosity of the Coralline Limestone ranges from 2 to 30% (Bonello, 1988).

Based on this characterization of limestones by previous researchers, the present study was carried out by a multidisciplinary team composed of geomorphologists, archaeologists, GIS scientists and geologists. The objective was to provide quantitative evaluations of the limestone loss having affected monuments of Malta and Gozo over the last half-millennium and to analyze differences between stone types. Study sites were selected among the coastal fortifications erected by the Knights of St John between 1530 and 1798, to protect Malta and Gozo from the expanding Ottoman Empire (Spiteri 2001).

2. Study sites and historical context

In order to measure limestone recession over the last half-millennium at the surface of Maltese fortifications erected by the Hospitaller Knights of the Order of St John, Structure from Motion (SfM) photogrammetry was carried out in six defensive structures that had undergone limited interventions or none, and still displayed original reference surfaces, i.e. zero datum levels. The test sites were selected based on their construction period, their homogeneous petrography and their accessibility. Extensively restored heritage buildings such as the Gozo Citadel and the Mdina and Vittoriosa fortifications were avoided, but selecting completely untouched defensive walls proved to be difficult due to the importance

of restoration works undertaken in the Maltese Islands in the 2000s-2010s (Spiteri, 2011). Of the six investigated ramparts, two are located in the Valletta Ditch, two in Fort St Elmo area and two at Fort Chambray in Gozo (Table 2).

The first study area is located in the Valletta defensive ditch (Fig. 4A and 5A-B), in the SW part of the Valletta fortified city. This walled city was designed by the Papal engineer Francesco Laparelli, and built in Globigerina Limestone between 1566 and 1570, just after the Great Siege of 1565 (Spiteri, 2001). The site for measuring limestone loss was selected in a non-restored part of the ditch, of particular interest because of its alternating *Franka* and *Soll* layers (determined visually), and of the remarkable preservation of original tooling marks in places. This part of the ditch wall faces the east. To make the comparison between stone materials easier, sections of the investigated photogrammetric imagery in *Franka* have been denominated Site 1 and sections in *Soll* appear as Site 2.

Site 3 is located in Abercrombie's Curtain. It is part of Fort St Elmo which is located at the NE tip of the Valletta fortified city (Fig. 4 and 5 C). The investigated section of fortifications faces the south-east direction and belongs to the external Carafa bastioned Enceinte designed by Don Carlos de Grunenbergh and built in 1687-89 on the foreshore surrounding the Fort to secure it (Spiteri, 2001). This curtain wall consists of Coralline Limestone. The lime mortar between ashlar blocks is barely visible for it has been eroded from the surface. No repointing of mortar joints had been done at the time of the study.

Site 4 is located in the NE part of the French Curtain, beneath Fort St Elmo (Fig. 4A and 5D). This curtain wall faces the north-west direction and was built in Globigerina Limestone in the

same period as the Carafa bastioned Enceinte (1687-1689), as documented by a plan drawn by the French military engineer Mederico Blondel (Spiteri, 2001, p. 260). The upper part of the wall had been subject to some modifications, possibly during the reign of Grand Master Pinto (1741-1773). In places, the surface of the ashlar blocks displays remnants of old lime render containing coarse sands. The characteristics of this material, which differ from recent lime renders, allow one to conclude that this material predates the mid-1870s, which is the period when cement was definitely in use in Malta (Cassar, 2010). It might have been applied in response to the rapid backweathering of the low quality Globigerina Limestone (*Soll* subtype) used as building stone at this site.

Sites 5 and 6 were selected at Fort Chambray, in the eastern part of the Island of Gozo (Fig. 4). The construction of this fortress overlooking Mgarr harbour has been retraced by Buhagiar and Cassar (2003) based on historic sources. Fort Chambray was designed in 1716 by the French military engineer Louis François d'Aubigné de Tigné, but due to a lack of funding, its construction was postponed until 1749. At that time, Jacques-François de Chambray, Governor of Gozo, financed the construction and preliminary excavations started based on Tigné's original design modified by Francesco Marandon. Work on the Fort itself began in 1752 and was completed by 1760. Stone quality was adjusted to strength requirements in the different parts of the Fortress: on the exposed external wall of the right ravelin (site 5 facing the north-west, Fig. 5E), a high quality Globigerina Limestone (*Franka*) was selected, whereas a lower quality Globigerina Limestone (*Soll*), more prone to honeycomb weathering, was used for the counterguard (site 6 facing the south-west, Fig. 5F). In both places, the surface of a number of stones has retained tooling marks. The original mortar has been partly eroded in

191 the counterguard and is therefore hardly visible at the surface. The external wall has been
192 recently repointed and currently displays light-coloured smooth joints of lime mortar.
193
194
195 ## 3. Methods
196
197 Methods combine stone-by-stone analysis of tool marks, photogrammetrical surveys and non-
198 destructive and non-invasive on-site hardness and contact sponge tests, aiming to
199 differentiate the stone materials of the investigated ramparts. Additionally, only a limited
200 number of laboratory analyses could be carried out due to sampling restrictions at heritage
201 sites.
202
203 ### 3.1. Identification of zero datum levels
204
205 At each site, the identification of tool marks allowed the inference of both the type of
206 stoneworking tools used for the construction and also to identify secure reference surfaces
207 according to the method used by André and Phalip (2010). These tentative reconstructions of
208 'zero datum levels' allowed the quantitative assessment of the amount of stone decay based
209 on photogrammetric methods.
210
211 ### 3.2. SfM photogrammetry
212

213 Structure from Motion (SfM) photogrammetry is an established and widely used method to
214 generate high resolution 3D scans, with applications in geoscience, archeoscience and cultural
215 heritage science (Smith et al., 2015; Historic England, 2017; McCarthy, 2014). This method,
216 which allows the obtaining of a high accuracy on weathered rock surfaces with areas < 10m² (Verma and Bourke, 2019), has already been used for the quantitative assessment of historical
217 (Verma and Bourke, 2019), has already been used for the quantitative assessment of historical
218 weathering rates in limestone monuments such as Mayan temples (Roussel and André, 2013).
219 In the present study, the close-range SfM method was used to produce high resolution 3D
220 models of representative areas of the weathering state (RAWS) of the ramparts, which
221 attributes are described in Table 2.
222
223 Photographs were collected with a Nikon D700 digital camera (12.0 megapixels) with a 35 mm
224 focal length lens to limit distortion effects. At each site, the RAWS was selected based on the
225 representativeness of the erosional processes observed on the fortified wall (above the rising
226 damp front), the necessity to avoid the occurrence of strong contrasts and the presence of
227 objects hindering the taking of photographs. A first series of photographs was taken
228 perpendicular to the ramparts, completed with a series of converging photographs. The
229 shooting distances ranged from 2 m to 6 m, depending on the area of the RAWS. Each point
230 within the RAWS was covered by at least five photographs to avoid the computation of
231 outliers. Scale bars (ruler or measuring tape) were set up around the study areas.
232
233 For each RAWS, data were processed as follows. The 3D reconstruction was performed
234 following the standard workflow of the Agisoft Photoscan Professional software (Westoby et
235 al., 2012; Agisoft 2014) to produce a dense coloured point cloud with a resolution depending
236 on the area of the RAWS, between 5 mm and 10 mm, and a scale bar error less than 3 mm.

237 This cloud was imported into the ArcGIS 10.2 software and converted into a digital elevation
238 model (DEM) in raster format (tiff) using ArcGIS 10.2. The reference surface (zero datum level)
239 was produced by selecting the points located in non-eroded areas of the dense cloud, some
240 of which exhibited original tooling marks. Selected points were then interpolated (with a linear
241 interpolation) to produce the reference surface raster. Reconstructing the reference surface
242 was not a straightforward process in severely weathered zones, where tool marks were hardly
243 visible. In these cases, protruding areas or 'hard points' were used to reconstruct a minimal
244 reference surface. For each RAWS, a model of stone recession since construction was
245 computed as the result obtained from the DEM raster being subtracted from the reference
246 surface raster. Finally, stone recession rates in mm/century ($mm.C^{-1}$) were computed as the
247 ratio between the recession model and the weathering period (Table 2).
248

249 ## 3.3. Contact sponge tests

250

251 On-site contact sponge tests were carried out to comparatively assess the water uptake
252 capacity of the different investigated limestone materials. This method, developed by Pardini
253 and Tiano (2004) is known to usefully complement the Karsten pipe and capillary rise methods
254 (Vandervoorde et al., 2009). It is a non-destructive, non-invasive and portable method which
255 consists of a 1034 Rodac contact-plate, 5.6 cm in diameter, containing a Calypso sponge which
256 is filled with approximately 7 g of water and weighed on a precision balance. The contact-plate
257 is pressed manually against the stone surface for a given time (30 or 60 seconds), and the
258 sponge is weighed again after this contact with the stone surface. The difference between
259 weights corresponds to the amount of water absorbed by the stone surface under test. Water
260 absorption is expressed in $g.m^{-2}.s^{-1}$. At each investigated site, three even-surfaced ashlar

blocks representative of the local petrography were selected. On each block, three contact sponge tests were performed, for a total of 54 tests carried out over the 6 investigated sites.

3.4. Hardness tests

Surface hardness measurements of limestone material were made on-site using an electronic rebound tester. The Proceq Equotip Piccolo 2 is a portable instrument, less destructive (impact energy less than 11.5 Nmm with the D probe) and as reliable as the Schmidt Hammer (Aoki and Matsukura, 2007; Viles *et al.*, 2011; Desarnaud *et al.*, 2019). Automatic compensation of impact direction allows measurements on vertical surfaces of the ashlars composing the investigated walls. Hardness values are directly readable on an LCD and are expressed in Leeb hardness using the D-probe (HLD) defined as the ratio of the rebound velocity to the impact velocity multiplied by 1000. At the six investigated sites, the hardness values were determined using the single impact (SIM) procedure (Desarnaud *et al.*, 2019): sole measurements were collected at individual points within a sample area to produce robust summary statistics. In this study, at least 20 individual measurements were made on 3 different ashlars for each study site. Overall, a total of 380 measurements were obtained to compare the hardness of the three limestone materials (*Franka*, *Soll* and Coralline limestone).

3.5. Laboratory analyses

Only four limestone samples detached from the investigated ramparts could be analyzed, including *Soll* and *Franka* Globigerina Limestones of Fort Chambray and the Valletta Ditch.

Sampling was impossible in the Fort St Elmo area: the detached *Soll* material of the French Curtain was too powdery to be sampled and the hard Lower Coralline Limestone of Abercrombie's Curtain did not provide any detached fragments. As two samples for *Franka* and *Soll* had been collected, for comparison two fragments of the Coralline Limestone blocks being used to repair the Gozo Citadel outer walls were also sampled.

To provide microscopic views of the limestone types and to realize petrographical analyses, plane sections were ground flat using SiC powders, and then polished by hand. Stone samples were cut to fit a 45x30 mm glass slide and impregnated with an epoxy resin under vacuum before making 30 µm thin sections. These were examined using an optical polarizing microscope (Olympus BX61) equipped with a camera (Qicam Fast 1394 color) linked to the sofware Saisam from Microvision instruments.

To assess the total porosity (*Pc*) and the pore access distribution of the stones, mercury intrusion porosimetry (MIP) was performed on samples of size 1 cm^3 with a Micromeretics AutoPore IV 9500. According to the method, the pore access radius measured by the instrument ranges from 200 µm (0.003 MPa) to 0.003 µm (207 MPa). Thus, pores of larger access radius such as macropores of 0.2 mm diameter and pores of smaller access radius of 0.003 µm were not taken into account. Spreading of the cumulative curve and thus heterogeneity of the material, can be defined by the scatter coefficient (C_d) calculated from a ratio of pores access radii (Wardlaw et al., 1988; Remy, 1993):

$$C_d = \frac{r_{20} - r_{80}}{r_{50}}$$

where r_{80}, r_{50} and r_{20} are the pore access radii allowing respectively the filling of 80, 50 and 20% of the porous network. If C_d<1, the pore distribution is concentrated around one pore radius, and a mean pore radius (Rm) for which the intrusive volume is maximal can be extracted from the incremental curve. If C_d>1, the pore distribution is spread. This means that the porous network is partitioned into several domains of different pore sizes (Remy, 1993) and no mean pore access radius can be determined by the incremental curve. The proportion of pore access larger than 1 µm and smaller than 1 µm was calculated to compare the results to previous studies (Cassar et al., 2002; Cassar et al., 2017; Zammit and Cassar, 2017).

3.6. Statistical analyses

As the distributions of stone recession rates, hardness and water absorption values were not normal, the non-parametric Kruskal-Wallis test and a post-hoc pairwise analysis (Dwass-Steel-Crichtlow-Fligner test) were used to assess the statistical significance of stone recession rates and of hardness and water absorption differences between the investigated materials. Moreover, following the recommendations of Mottershead (2000) and Wilhelm *et al.* (2016), median, median absolute deviation (MAD), the 5th and 95th percentiles were computed for stone recession rates, hardness and water absorption distributions as they are more robust summary statistics for non-normally distributed data (Filzmoser and Todorov, 2013). Additionally, 95% confidence intervals of summary statistics were estimated using a bootstrap technique (resampling with replacement, bootstrap samples = 1000).

4. Results

4.1. Identification of zero datum levels

Tool marks were sought to help to reconstruct the original surfaces and tentatively estimate the limestone loss since construction, based on photogrammetry. At Fort Chambray, both vertical and oblique marks left by toothed stone axes are preserved in the Globigerina Limestone on a number of ashlar blocks of the counterguard (Fig . 6A) and the right ravelin (Fig. 6C). In the Valletta Ditch, marks left by pickaxes are found very well preserved in many places on the high quality Globigerina Limestone (*Franka*) but not on the low quality *Soll* that outcrops as backweathered lenses within the *Franka* (Fig. 6B). The greatest difficulties were met in the St Elmo area. In Abercrombie's Curtain, the Coralline Limestone stone surface has retained very few tool marks, due to the abundance of Coralline algae which make the stone surface rough and irregular compared to the smooth surface of Globigerina Limestone. And in most of the French Curtain, the *Soll* material has been extensively subjected to backweathering, leaving very few intact stones which could have allowed the reconstruction of a reference surface. Although intra-burrow cemented material is often protruding (Fig. 6D), it has been itself subject to weathering and does not indicate the original top surface of the stonework. The zero datum level was therefore tentatively sought in the stones of the upper part of the French Curtain.

4.2. Weathering rates inferred from SfM photogrammetric analysis

Computing of 3D models of stone recession such as the one of Valletta Ditch presented in Fig. 7 has yielded median values of total stone recession since construction that are ranging from

4.1 mm to 179.8 mm (Table 3). Distributions of stone recession values exhibit two contrasting shapes (Fig. 8). The harder limestone types (Coralline Limestone and *Franka* facies of Globigerina Limestone) of sites 1, 3 and 5 show concentrated low values and a very low positive skewness of stone recession distributions (MAD < 4). On the contrary, the softer *Soll* facies of Globigerina Limestone of sites 2, 4 and 6 exhibit highly dispersed values (MAD ranging from 38.8 to 81.4) with a strong positive skewness.

Based on the duration of exposure of the investigated fortifications to the salt-laden corrosive atmosphere, the SfM data yielded median stone recession rates ranging from 1.2 mm to 60.7 mm/century (Fig. 9, top). The most resistant limestones, with recession rates ranging from 1.2 to 1.6 mm/century, were the high quality Globigerina Limestone (*Franka*) of the Valletta Ditch and Fort Chambray and the Coralline Limestone of Abercrombie's Curtain at St Elmo. By contrast, the low quality Globigerina Limestone (*Soll*) has been subject to rapid weathering, of 40.5 mm/century in the Valletta Ditch and 60.7 mm/century in the Fort Chambray Counterguard. The highest recession rates as expressed by the 95^{th} percentile confirm the high contrast between the resistant and the soft facies, with values of 3-10 mm/century for Coralline and *Franka* facies against 109-140 mm/century for *Soll* facies. As to the median recession rate of 21.5 mm/century obtained for the *Soll* of the French Curtain, this could be a questionable value that will be dealt with further in the discussion.

The Kruskal-Wallis test confirmed that the stone recession rates are significantly different (alpha=0.05; K= 203929256; P<0.0001). The post-hoc pairwise analysis (Dwass-Steel-Crichtlow-Fligner test) identified five different groups of stone recession rates among the six investigated sites. The first group gathers the undifferentiated lowest recessions rates of the

Coralline Limestone of site 3 (Fort St Elmo) and *Franka* Globigerina Limestone of site 1 (Valletta Ditch). The four last groups of stone recession rates contain one site each and are upwardly sorted as follows: The Globigerina *Franka* of site 5 (Fort Chambray), the Globigerina *Soll* of site 4 (French curtain), the Globigerina *Soll* of site 2 (Valetta Ditch), the Globigerina *Soll* of site 6 (Fort Chambray).

4.3. Stone characterization based on non-destructive on-site tests

The results of the contact sponge and surface hardness tests are summarized in Table 4 and Fig. 9. Contact sponge data indicate that the water uptake capacity of *Soll* was on average two to three times higher than that of *Franka* and Coralline Limestone (6.3 $g.m^{-2}.s^{-1}$ against 2.5 $g.m^{-2}.s^{-1}$). Interestingly, the water uptake capacities of *Franka* and Coralline Limestone are of the same order of magnitude at the investigated sites. The contrast between the two facies of Globigerina Limestones (*Franka* and *Soll*) is particularly striking for the highest values (2.7 against 14.6 $g.m^{-2}.s^{-1}$ for the centile 95^{th} at the five investigated sites). In the more resistant stone types (Coralline Limestone and *Franka*), data collected on three different stones for every site were quite similar, in sharp contrast with the results obtained for the friable *Soll* material. In particular, the three ashlar blocks tested for the *Soll* material of the French Curtain showed a marked variability in the values of water uptake capacity (MAD > 1.0) as expressed on boxplots (Fig. 9, middle).

The Kruskal-Wallis test confirmed that the water absorption of the tested materials was significantly different (alpha=0.05; K=40.449; P<0.0001; the p-value was calculated using

10,000 Monte Carlo simulations). The post-hoc pairwise analysis (Dwass-Steel-Crichtlow-Fligner test) identified three different groups of water absorption among the six investigated sites. The first group gathers the undifferentiated lowest water absorption values of the *Franka* Globigerina of site 1 (Valletta Ditch) and the Coralline Limestone of site 3 (Fort St Elmo). The second group contains only the *Franka* Globigerina Limestone of site 5 (Fort Chambray) characterized by intermediate water uptake values. The last group gathers the high values of water absorption of the *Soll* Globigerina Limestone of site 2 (Valetta Ditch), site 4 (French curtain) and site 6 (Fort Chambray).

Regarding the surface hardness recorded by the Equotip portable tester, the results clearly indicated a gradient in the mechanical resistance of the three tested stone materials (Table 4 and Fig. 9, bottom). The Coralline Limestone of St Elmo was by far the hardest material (434.5 HLD), followed by the *Franka* (365 and 276 HLD for sites 5 and 1). Last, the Soll was the least mechanically resistant material, with median values ranging from 172.5 to 269.0 HLD. Results of the Kruskal-Wallis test confirmed that the surface hardness of the tested materials was significantly different (alpha=0.05; K=278.34; P<0.0001). Moreover, the post-hoc pairwise analysis (Dwass-Steel-Crichtlow-Fligner test) identified five different groups of material hardness in the six investigated sites, from the softest *Soll* of the Valetta Ditch (site 2) to the hardest Coralline Limestone of Abercrombie's Curtain at Fort St Elmo (site 3). Whereas the surface hardness of *Franka* and *Soll* was significantly different at Fort Chambray and in the Valletta Ditch, the post-hoc analysis concluded an absence of hardness difference between the *Soll* of the French Curtain (site 4) and the *Franka* of the Valletta Ditch (site 1).

4.4. Stone characterization based on laboratory analyses

Thin sections allowed the differentiation of the three limestone types. The *Franka* facies of the Valletta Ditch is a fine-grained limestone displaying very small and well sorted bioclasts (<250 µm), mainly foraminifers such as *Globigerina*, and additional fragments of echinoderms (Fig. 10A). These small bioclasts are embedded within an abundant micritic and microsparitic matrix which reduces the macroporosity ; the Franka appears therefore as a mainly microporous and rather cohesive stone. By contrast, the *Soll* of the Valletta Ditch can be described as a non-cohesive bioclastic grainstone containing large benthic foraminifers and pelletoids (Fig. 10B). The macroporosity of this facies of Globigerina Limestone is high and well connected. This stone is poorly cemented by a sparse biomicritic material, and can be classified either as a biopelmicrite (Folk classification) or as a biopellitic wackestone (Dunham classification). The *Soll* sample of Fort Chambray, which is entirely microcracked, displays the same large benthic foraminifers as those of the Valletta Ditch. However, at Chambray, the bioclasts are embedded within a more abundant biomicritic matrix filling most of the macropores (Fig. 10C). Last, the thin sections of the Coralline Limestone sampled at Gozo Citadel (Fig. 10D) show large, heterogeneous and often broken bioclasts including echinoderms, foraminifers, coralline red algae and fragments of oyster shells. Fragmented echinoderms, including sea urchins, display at places rather large syntaxial sparitic cements. More importantly, the bioclasts of the Coralline Limestone are embedded within an heterogeneous biomicritic matrix which does not occlude all the intergranular macropores.

The results of the mercury intrusion porosimetry obtained for the three limestones types are summarized in Table 5 and Fig. 11. Values of total porosity (Pc) range from 20.5 to 37.5%. The two samples of Coralline Limestone, which were collected at the same site, provided

448 comparable values (20-22%). By contrast, the samples of Globigerina Limestone showed a
449 marked variability between sites, with values ranging from 27 to 37%. This variability was
450 observed both in *Franka* and *Soll*, with contrasted values between Fort Chambray and the
451 Valletta Ditch. Interestingly, at this last site, the mean pore radius (Rm), for which the intrusive
452 volume is maximal, allowed differentiation between the two lithofacies of Globigerina
453 limestone, with a Rm value 27 times higher in *Soll* than in *Franka*. Moreover, the analyses
454 indicated that both the Coralline Limestone and the *Soll* Globigerina Limestone were mainly
455 macroporous (64 to 79% pores >1µm), whereas *Franka* displayed up to 60% pores <1µm, with
456 a marked variability between sites.
457

458 ## 5. Discussion

459

460 Data computing of high-resolution 3D models of weathered fortifications obtained by SfM
461 photogrammetry has yielded median stone recession rates ranging from 1.2 to 60.7
462 mm/century, which should be considered as rough orders of magnitude. These quantitative
463 data allow fruitful comparisons between stone materials of the Maltese Islands, except in one
464 site, the French Curtain near Fort St Elmo, for which the quantitative results prove to be
465 unreliable. This is due to the uncertainties related to the reference surface reconstructed to
466 quantify the limestone recession. At this site, the generalized backweathering of the *Soll* ashlar
467 blocks has erased most tool marks. This has significantly reduced the number of reliable 'hard
468 points' which would have allowed the more certain reconstruction of the zero datum level.
469 Moreover, it seems that the backweathering of this rampart had started rapidly after
470 construction, requiring the application of lime render still visible at places. This application,
471 which predates the use of cement starting from the 1870s in Malta, has therefore reduced the

exposure time of the stone ashlars. As both the geometric reconstruction and the chronological control of the reference surface are uncertain, it seems appropriate not to take into consideration the recession value obtained for the French Curtain in the following discussion of quantitative results.

Based on the five remaining sites, the limestone durability scale can be expressed as follows : Coralline ≥ *Franka* >>> *Soll*. Both the Coralline Limestone and the high quality Globigerina Limestone (*Franka*) have yielded very low recession rates, between 1 and 2 mm/century. These results confirm the great durability of these building limestones, which is on the same order of magnitude as the one of the sparitic limestones used in the Vauban fortifications of the French Atlantic coast (Gruson, 2013). By contrast, the rapid recession rates obtained for *Soll* (40-60 mm/century) confirm the low durability of the *Soll* facies, as observed previously on abandoned quarry faces and through salt weathering tests (Cassar 2002, 2010; Fitzner et al., 1996; Rothert et al., 2007; Cassar et al., 2008; Zammit and Cassar, 2017). This soft subtype of Globigerina Limestone appears even more prone to decay than the micritic and platy limestones of the French Atlantic coast for which the maximum recession rates hardly reach 30 mm/century (Gruson, 2013).

As expressed in Fig. 12, the results of the on-site behaviour of the investigated limestones (water absorption and hardness), as well as their microscopic structure, shed some light on the controlling factors of their contrasted durabilities. *Soll*, which has yielded the fastest weathering rates is the least mechanically resistant material (median surface hardness below 230 HLD) and has the highest on-site water uptake capacity (median over 4.9 $g.m^{-2}.s^{-1}$). Moreover, microscopic observations indicate that it is a non-cohesive, poorly cemented or

496 microcracked biomicritic Globigerina Limestone. Conversely, *Franka*, which is the most
497 durable facies of Globigerina Limestone, presents a higher mechanical resistance (median
498 surface hardness ranging from 276 to 365 HLD) and a lower on-site water uptake capacity
499 (median values ranging from 1.8 to 3.6 $g.m^{-2}.s^{-1}$). The observation of thin sections shows that
500 it is a fine-grained and cohesive limestone of which small and well-sorted bioclasts are bound
501 together with an abundant micritic and microsparitic matrix. Last, the investigated facies of
502 Coralline Limestone, which is at least as durable as *Franka*, has a low on-site water uptake
503 capacity (1.8 $g.m^{-2}.s^{-1}$) and is by far the most mechanically resistant material (median surface
504 hardness of 434.5 HLD).
505
506 The results of the porosimetric analyses are more ambiguous. On the one hand, the values of
507 total porosity (20-22% for Coralline limestone and 27-37% for Globigerina limestones) fall
508 within the ranges of 2-30% and 24-41% provided by previous authors (Bonello, 1988; Cassar,
509 2002). On the other hand, the tendency of our samples of *Soll* to be more macroporous than
510 those of *Franka* does not fit with previous results showing that *Franka* displays predominantly
511 larger pores than *Soll* (Cassar, 2002; Rothert et al., 2007; Zammit and Cassar, 2017). However,
512 our results do not question these conclusions that are based on a much larger number of
513 samples from quarry faces, which has allowed the previous authors to minimize the effects of
514 the variability of porosimetric characteristics between sites and between samples. This
515 variability is known to be very high in the Globigerina Limestone which includes a variety of
516 subtypes (Diana et al., 2014). The small difference of hardness between the *Franka* of the
517 Valletta Ditch and the *Soll* of the French Curtain is another illustration of the complexity of the
518 Maltese Globigerina limestone lithofacies.
519

Concerning the much higher porosities of *Franka* and *Soll of* the Valletta Ditch than those measured on the samples from Fort Chambray, these might be explained by the longer exposure time in the Ditch (444 years against 254 years) and by the easier diffusion of water within the continuous limestone layers of the Ditch than in the ashlar masonry of Fort Chambray. Last, the unusually high variability of the water uptake capacity of the *Soll* material of the French Curtain, with values ranging from 2.4 to 16.1 $g.m^{-2}.s^{-1}$ might be explained by differing surface conditions occurring in different ashlar blocks (cf. the model of limestone weathering by Rothert et al. (2007), which includes episodes of surface hardening due to calcite migration). In the investigated sites, the highest water uptake capacity was found on blocks still displaying flaking features, whereas the stone material exposed after detachment of the flakes absorbed less water.

6. Conclusions

In the investigated Maltese fortifications, the present study provides novel quantitative data which highlights the existence of a two-rate weathering regime within the Globigerina Limestone types, the main building stone of the Maltese Islands. With a median stone recession of 1.4 mm/century against 50.6 mm/century, the cohesive subtype called *Franka* has resisted 36 times better to salt-laden atmospheric aggression than the non-cohesive *Soll* subtype. The Lower Coralline Limestone has also resisted quite well, with a stone recession of 1.3 mm/century, on the same order of magnitude as *Franka*. These quantitative results are in line with the two-rate weathering regime found for eight limestone types within fortifications of the French Atlantic coast. With 2.4 mm/century against 17.9 mm/century, the sparitic

544 limestones are on average 7 times more durable than the micritic and platy limestones
545 (Gruson, 2013). The contrast between durable and fragile limestones is therefore five times
546 less pronounced on the Atlantic coast than in the Maltese Islands. It is probably due to the
547 high susceptibility to powdering of the Maltese *Soll* facies of Globigerina Limestone which has
548 no equivalent on the Atlantic coast.
549
550 Regarding the controlling factors of the two-rate weathering regime, the on-site contact
551 sponge tests reveal that the median water uptake capacity of the least durable limestone (*Soll*)
552 is on average two to three times higher than that of *Franka* and Coralline Limestone (5.4 to
553 5.9 $g.m^{-2}.s^{-1}$ against 1.8 to 3.6 $g.m^{-2}.s^{-1}$). The correlation of limestone durability with surface
554 hardness is not as straightforward as with water absorption. There is a decreasing gradient in
555 the median values of mechanical resistance of the three tested materials, with 434.5 HLD for
556 the Coralline Limestone, 316 HLD for the *Franka* and 228 HLD for the *Soll*. If this last facies is
557 both the least durable and the least mechanically resistant, the two other limestones, which
558 have similar durabilities, have significantly different hardness. This result could be interpreted
559 as a compensation of a lower hardness by a better capacity to allow water circulation and
560 therefore moisture wicking, but it is quite clear that other controlling factors do exist.
561 Microscopic examinations have revealed differences in cohesiveness between the durable
562 *Franka* and the friable *Soll*: whereas the bioclasts of the first facies were bound together by
563 an abundant micritic and microsparitic matrix, the second facies was poorly-cemented or
564 microcracked. But additional controls should be explored, such as the abundance and nature
565 of the insoluble residue, which might be an important controlling factor of varying durability
566 as suggested by Cassar (1999) and Zammit and Cassar (2017).
567

Further research should be based on a larger number of sites and of representative areas of the weathering state (RAWS) of ramparts and comparisons with fresh quarry samples. Moreover, the implementation of the on-site tests should be based on a refined methodology: the surface conditions of the tested ashlar blocks should be taken into account for they impact their water uptake capacity. Last, additional laboratory analyses should be carried out, with special reference to the identification of the nature of the insoluble residue including the clay content. Such an improved methodology applied to additional sites should allow to refine the quantitative estimates and the limestone durability scale inferred from the present study.

Acknowledgements

The authors express their gratitude to Prof. Jean-Philippe Luis, Director of the Maison des Sciences de l'Homme of Clermont-Ferrand, for his financial support. Fruitful exchanges have been held with distinguished members of Heritage Malta, the National Agency in charge of the Maltese cultural heritage: Ivan Barbara (Estate Manager), Kenneth Gambin (then Chief Executive Officer) and Godwin Vella (then Head of the Curatorial Section). Thanks are also due to Fr. Anthony Mizzi and Fr. Michael Curmi who provided detailed information about the history of the statues of Parish Church St Margaret, in Sannat, Gozo.

References

Agisoft, 2014. Agisoft LLC, Agisoft PhotoScan user manual: professional edition, V.1.1, 85 p.

André, M.F., Phalip, B., 2010. Rates of stone recession on Mediaeval monuments: some thoughts and methodological perspectives. Cadernos do Laboratorio xeoloxico de Laxe, A Coruña, 35, 13-40. ISSN: 0213-4497

Aoki, H., Matsukura, Y., 2007. A new technique for non-destructive field measurement of rock-surface strength: an application of the Equotip hardness tester to weathering studies. Earth Surface Processes and Landforms, 32, 1759-1769. https://doi.org/10.1002/esp.1492

Augeyre, M., 2006. La dégradation du patrimoine funéraire calcaire sur le littoral atlantique français : l'exemple de l'île de Ré. Master's thesis, Université Blaise Pascal, Clermont-Ferrand (109 pp.).

Augeyre, M., 2008. La dégradation du patrimoine funéraire calcaire sur le littoral atlantique français : l'exemple de l'île de Ré. Bulletin de l'Association de Géographes Français, 1, 63-70. https://doi.org/10.3406/bagf.2008.2599

Bonello, S., 1988. Engineering properties of rocks and soils of the Maltese Islands. B.E. & A. dissertation, University of Malta.

Bowen Jones, H., Dewdney, J.C., Fisher, W.B., 1961. Malta: a background for development. Durham University Press, Durham (356 pp.).

Buhagiar, K., 2007. Water management strategies and the case-dwelling phenomenon in late-medieval Malta. Medieval Archaeology, 51, 103-131. https://doi.org/10.1179/174581707x224688

Buhagiar, K., Cassar, J., 2003. Fort Chambray: the genesis and realisation of a project in eighteen century Malta. Melita Historica, 13 (4), 347-364.

618 Cassar, J., 2002. Deterioration of the Globigerina Limestone of the Maltese Islands, in: Siegesmund, S.,
619 Weiss, T., Vollbrecht, A. (Eds), Natural stone, weathering phenomena, conservation strategies and case
620 studies. Geological Society London, Special Publication, 205, 33-49.
621 http://dx.doi.org/10.1144/GSL.SP.2002.205.01.04
622
623 Cassar, J., 2004. Composition and property data of Malta's building stone for the construction of a
624 database, in: Přikryl, R., Siegl, P. (Eds), Architectural and sculptural stone in cultural landscape. The
625 Karolinum Press, Prague, 11-28.
626
627 Cassar, J., 2010. The use of limestone in a historic context – the experience of Malta, in: Smith, B.J.,
628 Gomez-Heras, M., Viles, H.A., Cassar, J., Eds, Limestone in the built environment. Geological Society
629 London, Special Publication, 331, 13-25.
630 https://www.um.edu.mt/library/oar//handle/123456789/12228
631
632 Cassar, J., Cefai, S., Grima, R., Stroud, K., 2018. Sheltering archaeological sites in Malta: lessons learnt.
633 Heritage Science, 6 (36).https://doi.org/10.1186/s40494-018-0201-6
634
635 Cassar, J., Galea, M., Grima, R., Stroud, K., Torpiano, A., 2011. Shelters over the Megalithic Temples of
636 Malta: debate, design and implementation. Environ. Earth Sci., 63, 1849-1860.
637 https://doi.org/10.1007/s12665-010-0735-8
638
639 Cassar, J., Marrochi, A., Santarelli, M.L., Muscat, M., 2008. Controlling crystallization damage by the
640 use of salt inhibitors on Malta's limestone. Materiales de Construcción, 58 (289-290), 281-293.
641 https://doi.org/10.3989/mc.2008.v58.i289-290.83
642

643 Cassar, J., Torpiano, A., Zammit, T., Micallef, A., 2017. Proposal for the nomination of Lower
644 Globigerina Limestone of the Maltese Islands as a « Global Heritage Stone Resource ». Episodes, 40
645 (3), 221-231. https://dx.doi.org/10.18814/epiiugs/2017/v40i3/017025
646
647 Cooke, R.U., Inkpen, R.J., Wiggs, G.F.S., 1995. Using gravestones to assess changing rates of weathering
648 in the United Kingdom. Earth Surface Processes and Landforms, 20, 531-546.
649 https://doi.org/10.1002/esp.3290200605
650
651 Desarnaud, J., Kiriyama, K., Bicer Simsir, B., Wilhelm, K., Viles, H.A., 2019. A laboratory study of Equotip
652 surface hardness measurements on a range of sandstones: what influences the values and what do
653 they mean? Earth Surface Processes and Landforms, 44 (7), 1419-1429.
654 https://doi.org/10.1002/esp.4584
655
656 Diana, G., Cassar, J ., Zammit, G., 2014. Physical characteristics of Globigerina Limestone using
657 ultrasonic and thermographic methods. Quarterly Journal of Engineering Geology and Hydrogeology,
658 47, 251-257. https://doi.org/10.1144/qjegh2013-066
659
660 Filzmoser, P., Todorov, V., 2013. Robust tools for the imperfect world. Information Sciences, 245, 4–
661 20. https://doi.org/10.1016/j.ins.2012.10.017
662
663 Fitzner, B., Heinrichs, K., Volker, M., 1996. Model for salt weathering at Maltese Globigerina Limestone,
664 in: Zezza, F. (Ed.), Origin, mechanisms and effects of salt on degradation of monuments in marine and
665 continental environments. Proceedings, European commission research workshop on protection and
666 conservation of the European cultural heritage, Bari, Italy, Research Report, 4, 331-344.
667 https://www.um.edu.mt/library/oar/handle/123456789/12229
668

669 Gatt, P.A., 2006. Model of limestone weathering and damage in masonry: sedimentological and
670 geotechnical controls in the Globigerina Limestone formation (Miocene) in Malta. Xjenza, 11, 30-38.
671 https://www.um.edu.mt/library/oar//handle/123456789/12167
672
673 Geikie, A., 1880. Rock weathering, as illustrated in Edinburgh churchyards. Proceedings of the Royal
674 Society of Edinburgh, 10, 518-532. https://doi.org/10.1017/S0370164600044242
675
676 Gruson, S., 2013. Vitesses de détérioration des calcaires monumentaux des sites fortifiés du littoral
677 charentais. Master's thesis, Université Blaise Pascal, Clermont-Ferrand, 149 p.
678
679 Historic England, 2017. Photogrammetric applications for cultural heritage. Guidance for good
680 practice. Report HEAG066, Historic England, Swindon, United Kingdom.
681 https://historicengland.org.uk/images-books/publications/photogrammetric-applications-for-
682 cultural-heritage/heag066-photogrammetric-applications-cultural-heritage/
683
684 Inkpen, R.J., Jackson, J., 2000. Contrasting weathering rates in coastal, urban and rural areas in
685 southern Britain: preliminary investigations using gravestones. Earth Surface Processes and Landforms,
686 25, 229-238. https://doi.org/10.1002/(SICI)1096-9837(200003)25:3<229::AID-ESP52>3.0.CO;2-Y
687
688 McCarthy, J., 2014. Multi-image photogrammetry as a practical tool for cultural heritage survey and
689 community engagement. Journal of Archaeological Science, 43, 175-185.
690 https://doi.org/10.1016/j.jas.2014.01.010
691
692 Meierding, T.C., 1993. Inscription legibility method for estimating rock weathering rates.
693 Geomorphology, 6, 273-286. https://doi.org/10.1016/0169-555X(93)90051-3
694

Mottershead, D.N., 2000. Weathering of coastal defensive structures in southwest England: a 500 year stone durability trial. Earth Surface Processes and Landforms, 25, 1143–1159. https://doi.org/10.1002/1096-9837(200009)25:10<1143::AID-ESP129>3.0.CO;2-N

Pardini, C., Tiano, P. 2004. Valutazione *in situ* dei trattamenti protteviti per il materiale lapideo. Proposta di una nuova semplice metodologia. Arkos, 5, 32-38.

Pedley, H. M., House, M. R., Waugh, B., 1976. The Geology of Malta and Gozo. Proc. Geol. Ass., 87 (3), 325-341. https://doi.org/10.1016/S0016-7878(76)80005-3

Remy, J.M., 1993. Influence de la structure du milieu poreux carbonaté sur les transferts d'eau et les changements de phase eau-glace. Application à la durabilité au gel de roches calcaires de Lorraine. Phd Thesis, Institut national polytechnique de Lorraine, Nancy (327 pp.).

Rothert, E., Eggers, T., Cassar, J., Ruedrich, J., Fitzner, B., Siegesmund, S., 2007. Stone properties and weathering induced by salt crystallization of Maltese Globigerina limestone, in: Přikryl, R., Smith, B.J., Eds, Building stone decay: from diagnosis to conservation. Geological Society London, Special Publication, 271, 189-198. https://doi.org/10.1144/GSL.SP.2007.271.01.19

Roussel, E., André, M.F., 2013. Quantitative assessment of pre- and post-restoration weathering rates of limestone Mayan temples (Uxmal, Yucatán). Supplementi di Geografia Fisica e Dinamica Quaternaria 36 (1):169-179. DOI 10.4461/GFDQ.2013.36.14

Smith, B.J., Gomez-Heras, M., Viles, H.A., Cassar, J., Eds, 2010. Limestone in the built environment. Geological Society London, Special Publication, 331, (257 pp.). https://doi.org/10.1144/SP331

721 Smith, M., Carrivick, J., Quincey, D., 2015. Structure from Motion Photogrammetry in physical
722 geography. Progress in Physical Geography, 40 (2), 247-275.
723 https://doi.org/10.1177/0309133315615805
724
725 Spiteri, S.C., 2001. Fortresses of the Knights. Book Distributors Limited, Malta (384 pp.).
726
727 Spiteri, S.C., 2008. The art of fortress building in Hospitaller Malta. BDL Publishing, Malta.
728
729 Spiteri, S.C., 2011. Avec l'aide de l'Union Européenne, Malte restaure ses fortifications. In Situ Revue
730 des Patrimoines, 16. https://doi.org/10.4000/insitu.333
731
732 Torfs, K., van Grieken, R., Cassar, J., 1996. Environmental effects on deterioration of monuments: case
733 study of the Church of Sta. Marija Ta' Cwerra, Malta. In Proc. EC Research Workshop on Origin,
734 Mechanisms and Effects of Salts on Degradation of Monuments in Marine and Continental
735 Environment, ed. F. Zezza, pp. 441-451. Tecnomack, Bari."
736 https://www.um.edu.mt/library/oar/handle/123456789/59917
737
738 Vandervoorde, D., Pamplona, M., Schalm, O., Vanhellemont, Y., Cnuddle, V.,Verhaeven, E., 2009.
739 Contact sponge method: Performance of a promising tool for measuring the initial water absorption.
740 Journal of Cultural Heritage, 10, 41-47. https://doi.org/10.1016/j.culher.2008.10.002
741
742 Vannucci, S., Alessandrini, G., Cassar, J., Tampone, G., Vannucci, M.L., 1994. The prehistoric, megalithic
743 temples of the Maltese Islands: causes and processes of deterioration of Globigerina Limestone, in:
744 Fassina, V., Ott, H., Zezza, F. (Eds), Proceedings of the Third International Symposium on the
745 Conservation of Monuments in the Mediterranean Basin, Venice, Italy, 22 – 25 June 1994, 555-565.
746

747 Verma, A. K., Bourke, M. C., 2019. A method based on structure-from-motion photogrammetry to
748 generate sub-millimetre-resolution digital elevation models for investigating rock breakdown features.
749 Earth Surface Dynamics, 7, 45–66. https://doi.org/10.5194/esurf-7-45-2019
750
751 Viles, H., Goudie, A., 1992. Weathering of limestone columns from the Weymouth seafront, England.
752 Proceedings 7th International Congress on Deterioration and Conservation of Stone, Lisbon, June 1992,
753 297-304.
754
755 Viles, H., Goudie, A., Grab, S., Lalley, J. 2011. The use of the Schmidt Hammer rand Equotip for rock
756 hardness assessment in geomorphology and heritage science: a comparative analysis. Earth Surface
757 Processes and Landforms, 36, 320-333. https://doi.org/10.1002/esp.2040
758
759 Wardlaw, N.C., McKellar, M., and Yu, L., 1988. Pore and throat size distribution determined by mercury
760 porosimetry and by direct observation. Carbonates and Evaporites, 3, 1-16.
761 https://doi.org/10.1007/BF03174408
762
763 Westoby, M., Brasington, J., Glasser, N., Hambrey, M., Reynolds, J., 2012. 'Structure-from-Motion'
764 photogrammetry: A low-cost, effective tool for geoscience applications. Geomorphology, 179, 300-
765 314. https://doi.org/10.1016/j.geomorph.2012.08.021
766
767 Wilhelm, K., Viles, H., Burke, Ó. 2016. Low impact surface hardness testing (Equotip) on porous surfaces
768 - advances in methodology with implications for rock weathering and stone deterioration research:
769 Equotip Hardness Testing on Porous Rock and Stone. Earth Surface Processes and Landforms, 41,
770 1027–1038. https://doi.org/10.1002/esp.3882
771

772 Zammit, C., Cassar, J., 2017. Investigating possible correlations between the porosimetry and insoluble
773 residue content of Malta's Lower Globigerina Limestone. Bulletin of Engineering Geology and the
774 Environment, 76, 59-70. https://doi.org/10.1007/s10064-015-0817-7

775

776 LIST OF TABLES

777

778 Table 1. Historical limestone recession rates published by previous authors for European
779 coastal monuments.

780

781 Table 2. Selected attributes of the representative areas of the defensive structures to quantify
782 by SfM photogrammetry the limestone loss in sites in Malta (sites 1-4) and Gozo (sites 5-6).
783 The aspect column indicates the compass direction that the rampart faces.

784

785 Table 3. Limestone recession rates inferred from SfM photogrammetry.

786

787 Table 4. Summary statistics of water absorption and surface hardness of limestone materials
788 measured *in situ*. Bootstrapped upper and lower limits of 95% confidence interval are
789 indicated in italics.

790

791 Table 5. Results of the porosimetric analyses of the three investigated limestone types. Pc is
792 the total porosity, Rm the mean radius corresponding to the maximal intrusive volume, Cd is
793 the dispersion coefficient giving the degree of heterogeneity of the pore access distribution.

794

795

796 LIST OF FIGURES

797

798 Fig. 1. Severely alveolized statue of Saint Paul carved in the Globigerina Limestone by the
799 Sicilian sculptor Francesco Latulco around 1890 at St. Margaret Church, Sannat, Island of Gozo.
800 (Photo E. Roussel).

801

802 Fig. 2. External wall of Inquisitor's Palace in Vittoriosa showing individual blocks of Globigerina
803 Limestone at different stages of alveolar weathering, from almost sound stone to totally
804 backweathered stone (Photo M.F. André). Numbers indicate the phases of the damage model:
805 1 - non-weathered stone surface; 2 – local backweathering; 3 - cavities formation and salt
806 accumulation behind the crust; 4 - cavities coalescence and formation of larger and deeper
807 alveoli; 5 - pronounced backweathering results in the development of a more or less plain
808 surface and the rounding of block edges.

809

810 Fig. 3. Geological map of the Maltese Islands showing the investigated sites (adapted by
811 Bonello from Bowen Jones et al. 1961 and Buhagiar 2007, in Cassar 2010; adapted also from
812 the geological map available at continentalshelf.gov.mt).

813

814 Fig. 4. Maps of Valletta and Chambray fortifications showing the location of the investigated
815 ramparts in Malta and Gozo.
816 (source: https://en.wikipedia.org/wiki/File:Valletta_fortifications_map.png ;
817 https://en.m.wikipedia.org/wiki/File:Fort_Chambray_map.png)

818

819 Fig. 5. Views of the investigated defensive structures: Valletta Ditch (A-B), Abercrombie's
820 Curtain at Fort St Elmo (C), French Curtain behind Fort St Elmo (D), Right ravelin of Fort
821 Chambray (E), and Counterguard of Fort Chambray (F). Photos M.F. André and E. Roussel.
822
823 Fig. 6. Tool marks used to reconstruct zero datum levels to quantitatively assess the limestone
824 loss by SfM photogrammetry on the Fort Chambray counterguard (A), the Valletta Ditch (B)
825 and the Fort Chambray right ravelin (C). In addition, Fig 6D shows the intra-burrow cemented
826 material protruding from the soft Globigerina limestone of the French Curtain. Photos M.F.
827 André, E. Roussel, O. Voldoire.
828
829 Fig. 7. A 3-D model obtained by SfM photogrammetry showing the preferential stone
830 recession of the lenticular layers of *Soll* interstratified within the more resistant *Franka* facies
831 of Globigerina limestone in the Valletta Ditch.
832
833 Fig. 8. Histogram plots of stone recession since construction (in mm) for the six investigated
834 sites.
835
836 Fig. 9. Boxplots of stone recession rates (top), water absorption (middle) and surface hardness
837 (bottom) for the six investigated sites.
838
839 Fig. 10. Thin sections of the Globigerina and Upper Coralline limestone types of Malta and
840 Gozo: Franka, Valletta Ditch (A), Soll, Valletta Ditch (B), Soll, Fort Chambray counterguard (C),
841 Coralline limestone, Gozo Citadel (D). Photos G. Fronteau.
842

843 Fig. 11. Pore access distribution of the different limestones.

844 *Soll* and *Franka* are the Globigerina limestone samples and Coralline 1-2 are the Upper
845 Coralline limestone samples.

846

847 Fig. 12. Limestone durability scale obtained from data collected at 5 sites investigated in the
848 Valletta Ditch, Fort St Elmo (in Malta) and Fort Chambray (in Gozo)

849

Table 1

Table 1

Location	Monument Type	Limestone Type	Building Date	Weathering Period (yr)	Recession Rates (mm/century)			Source *(method)*
					min	mean	max	
Weymouth, S UK	Carlton Hotel (columns)	oosparitic	1860	135		2.0* 4.0**		Viles & Goudie 1992 *(carpenter's profile gauge)*
Ré Island, W France	Tombstones Ars-en-Ré (21)	sparitic	1808-1932	73-197	0.00	1.64	32.8	Augeyre 2006, 2008 *(plexiglass grid and metal ruler)*
	Tombstones La Couarde (11)	sparitic	1878-1925	80-127	0.00	1.78	31.5	
	Tombstones Le Bois-Plage (28)	sparitic	1867-1927	78-138	0.00	3.64	113.9	
	Tombstones St. Martin (25)	sparitic	1840-1933	72-165	0.00	1.77	21.7	
	Fortifications	micritic	1682	331	1.78	5.60	11.70	Gruson 2013 *(multi-image photogrammetry)*
	Fortifications	sparitic	1682	331	0.43	1.92	7.54	
	Church wall	sparitic	1862	151	0.36	3.81	18.86	
Oléron Island, W France	Fortifications	sparitic	1675	338	0.91	3.42	10.07	
	Fortifications	platy	1675	338	2.50	7.08	20.94	
	Church	sparitic	1703	310	0.41	3.16	14.97	
La Rochelle, W France	Fortifications	sparitic	1568	445	0.33	2.40	5.75	
	District Court	sparitic	1784	229	0.17 0.79	1.63* 4.90**	4.70 9.78	
Brouage, W France	Church wall	sparitic	1608	405	0.62	1.59	3.33	
	Bastions	sparitic	1635	378	0.05	2.53	8.57	
	Enclosure	sparitic	1853	160	0.95	3.29	10.22	
	Enclosure	platy	1853	160	8.00	28.85	54.67	
Esnandes, W France	Church (W portal)	sparitic	1150	863	0.00	1.59	4.68	
	Church (W portal restored)	sparitic	1885	128	0.00	1.53	4.55	
	Church (restored walls)	sparitic	1883	130	1.48	2.81	7.80	

*sheltered from sea spray **exposed to sea spray

TABLE 2

SITE ID	LOCATION	ARCHITECTURAL ELEMENT	BUILDING PERIOD	LIMESTONE TYPE	ASPECT	DISTANCE TO SEA (m)	SURFACE AREA (m^2)
1	SW Valletta walled city	Ditch counterguard	1566-1570	Globigerina/*Franka*	E	255	33.32
2	SW Valletta walled city	Ditch counterguard	1566-1570	Globigerina/*Soll*	E	255	29.50
3	E Fort St Elmo	Abercrombie's curtain	1687-1689	Coralline	SE	12	2.71
4	SW Fort St Elmo	French curtain	1687-1689	Globigerina/*Soll*	NW	25	15.99
5	N Fort Chambray, Gozo	Right ravelin	1749-1760	Globigerina/*Franka*	NW	360	2.35
6	N Fort Chambray, Gozo	Counterguard	1749-1760	Globigerina/medium quality	SW	420	4.49

Table 3

	Total stone recession since construction (mm)				*Weathering Period (yr)*	*Stone recession rates (mm/century)*			
	5th	***Median***	***MAD***	***95th***		***5th***	***Median***	***MAD***	***95th***
Site 1 - Valletta Ditch-Globigerina/*Franka*	0.3 *(0.31 ; 0.36)*	5.1 *(4.98 ; 5.25)*	4.0 *(3.89 ; 4.12)*	43.9 *(42.8 ; 45.01)*	444	0.1 *(0.07 ; 0.08)*	1.2 *(1.12 ; 1.18)*	0.9 *(0.87 ; 0.92)*	9.9 *(9.64 ; 10.13)*
Site 2 - Valletta Ditch-Globigerina/*Soll*	59.2 *(58.38 ; 60.04)*	179.8 *(177.83 ; 181.76)*	81.4 *(79.6 ; 83.1)*	484.6 *(479.33 ; 489.81)*	444	13.3 *(13.14 ; 13.52)*	40.5 *(40.05 ; 40.93)*	18.3 *(17.93 ; 18.71)*	109.1 *(107.95 ; 110.31)*
Site 3 - Fort St Elmo-Coralline	0.3 *(0.31 ; 0.36)*	4.2 *(4.14 ; 4.34)*	3.0 *(2.88 ; 3.04)*	20.4 *(19.86 ; 20.87)*	325	0.1 *(0.09 ; 0.11)*	1.3 *(1.27 ; 1.33)*	0.9 *(0.88 ; 0.93)*	6.3 *(6.11 ; 6.42)*
Site 4 - French Curtain-Globigerina/*Soll*	5.2 *(4.94 ; 5.42)*	69.9 *(69.21 ; 70.53)*	38.8 *(38.36 ; 39.27)*	177.2 *(175.97 ; 178.45)*	325	1.6 *(1.52 ; 1.67)*	21.5 *(21.29 ; 21.70)*	11.9 *(11.80 ; 12.08)*	54.5 *(54.14 ; 54.90)*
Site 5 - Fort Chambray-Globigerina/*Franka*	1.5 *(1.43 ; 1.51)*	4.1 *(4.08 ; 4.14)*	1.2 *(1.15 ; 1.18)*	7.7 *(7.62 ; 7.85)*	254	0.6 *(0.56 ; 0.59)*	1.6 *(1.6 ; 1.63)*	0.5 *(0.45 ; 0.46)*	3.0 *(3 ; 3.09)*
Site 6 - Fort Chambray-Globigerina/*Soll*	26.5 *(25.54 ; 27.48)*	154.1 *(152.68 ; 155.54)*	65.5 *(64.81 ; 66.08)*	357.0 *(353.64 ; 360.3)*	254	10.4 *(10.05 ; 10.82)*	60.7 *(60.11 ; 61.23)*	25.8 *(25.51 ; 26.01)*	140.5 *(139.23 ; 141.85)*

Table 3

	Water absorption (g.m-2.s-1)				***Hardness (Leeb hardness units)***			
	5th	***Median***	***MAD***	***95th***	***5th***	***Median***	***MAD***	***95th***
Site 1 - Valletta Ditch-Globigerina/*Franka*	1.1 *(0.83 ; 1.41)*	1.8 *(1.26 ; 2.38)*	0.4 *(0.04 ; 0.79)*	2.7 *(1.88 ; 3.61)*	186.0 *(168.42 ; 203.57)*	276.0 *(252.75 ; 299.24)*	53.5 *(39.82 ; 67.17)*	434.8 *(400.31 ; 469.18)*
Site 2 - Valletta Ditch-Globigerina/*Soll*	3.6 *(2.33 ; 4.81)*	5.4 *(4.27 ; 6.52)*	1.0 *(0.29 ; 1.66)*	7.1 *(6.23 ; 7.89)*	122.0 *(113.32 ; 130.67)*	172.5 *(158.35 ; 186.64)*	25.0 *(17.53 ; 32.46)*	245.1 *(229.09 ; 261.1)*
Site 3 - Fort St Elmo-Coralline	1.0 *(0.85 ; 1.1)*	1.8 *(0.5 ; 3)*	0.8 *(0.21 ; 1.32)*	3.0 *(2.81 ; 3.2)*	336.0 *(314.95 ; 356.94)*	434.5 *(410.81 ; 458.18)*	46.0 *(29.66 ; 62.33)*	578.4 *(543.23 ; 613.56)*
Site 4 - French Curtain-Globigerina/*Soll*	2.6 *(2.13 ; 3.01)*	4.9 *(0 ; 10.58)*	2.3 *(-1.62 ; 6.24)*	14.6 *(9.01 ; 20.21)*	214.8 *(199.81 ; 229.78)*	269.0 *(260.75 ; 277.24)*	14.5 *(6.71 ; 22.28)*	307.6 *(279.83 ; 335.36)*
Site 5 - Fort Chambray-Globigerina/*Franka*	3.0 *(2.56 ; 3.38)*	3.6 *(2.94 ; 4.35)*	0.4 *(0.01 ; 0.82)*	4.4 *(3.96 ; 4.89)*	246.9 *(213.08 ; 280.61)*	365.0 *(345.36 ; 384.63)*	46.5 *(33.95 ; 59.04)*	446.6 *(420.13 ; 473.06)*
Site 6 - Fort Chambray-Globigerina/*Soll*	4.4 *(3.43 ; 5.38)*	5.9 *(3.1 ; 8.67)*	1.5 *(0.5 ; 2.58)*	8.8 *(8.01 ; 9.66)*	147.8 *(117.22 ; 178.27)*	230.0 *(218.13 ; 241.86)*	30.0 *(19.15 ; 40.84)*	302.2 *(280.53 ; 323.76)*

Table 4

Table 5

Stone type	Globigerina / *Franka*		Globigerina / *Soll*		Coralline	
Sample	MT15	MT28	MT13	MT27	MT18	MT21a
Site location	Fort Chambray	Valletta Ditch	Fort Chambray	Valletta Ditch	Gozo Citadel	Gozo Citadel
Pc (%)	26.9	32.8	29.2	37.5	22.1	20.5
Rm (µm)	/	1.4	/	38.5	/	/
Cd	8.7	1.5	4.2	1.9	3.0	2.0
Pores<1 µm	46%	60%	36%	21%	25%	25%
Pores>1µm	54%	40%	64%	79%	75%	75%

Figure1

Click here to access/download;Figure (Color);FIG_1.JPG

Figure 2

Click here to access/download;Figure (Color);FIG_2.jpg

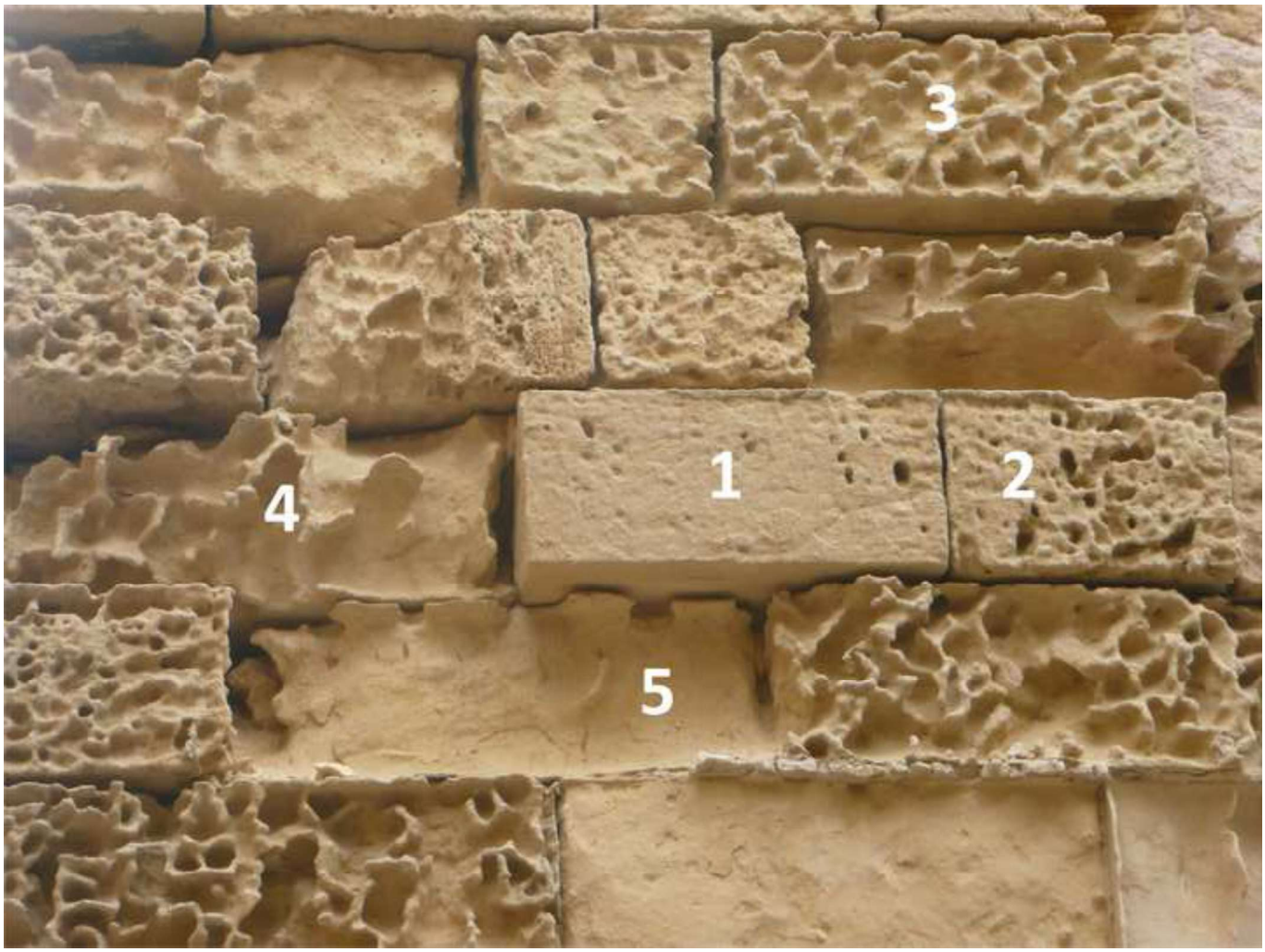

Figure 3

Click here to access/download;Figure (Color);FIG_3.jpg

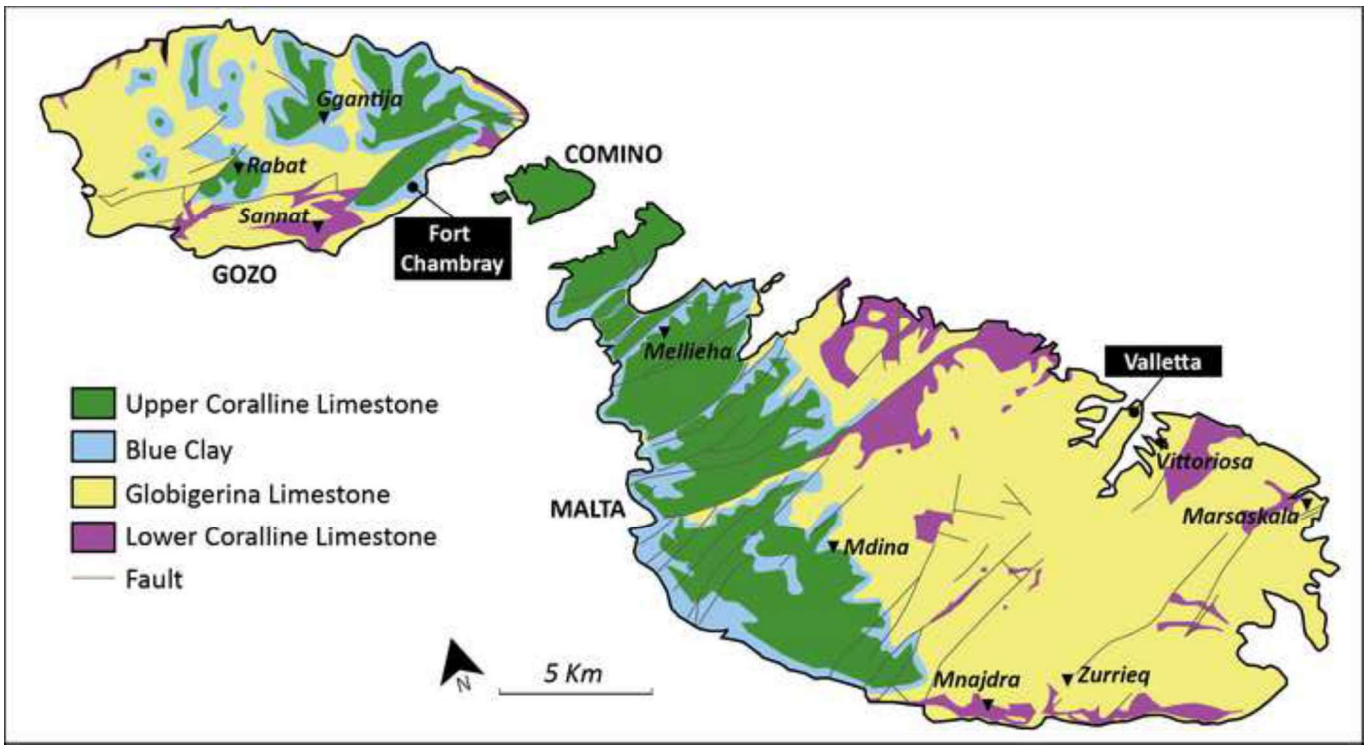

Figure 4

Click here to access/download;Figure (Color);FIG_4.jpg

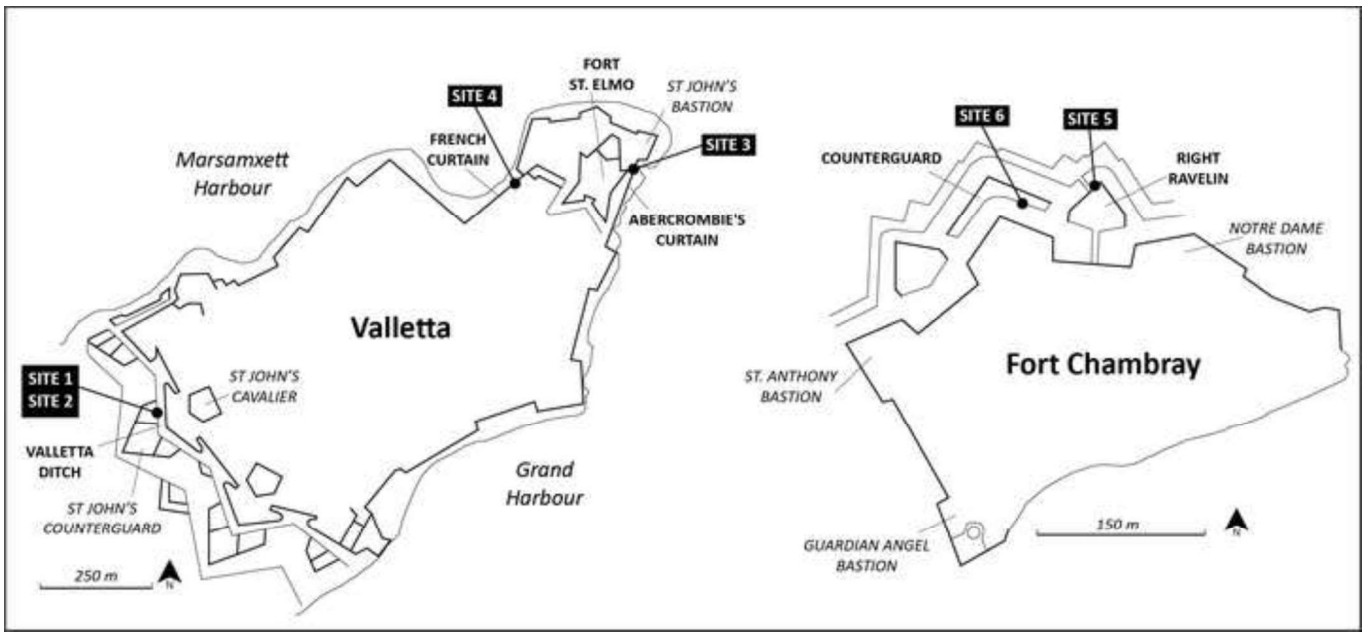

Figure 5

Click here to access/download;Figure (Color);FIG_5.jpg

Figure 6

Click here to access/download;Figure (Color);FIG_6.jpg

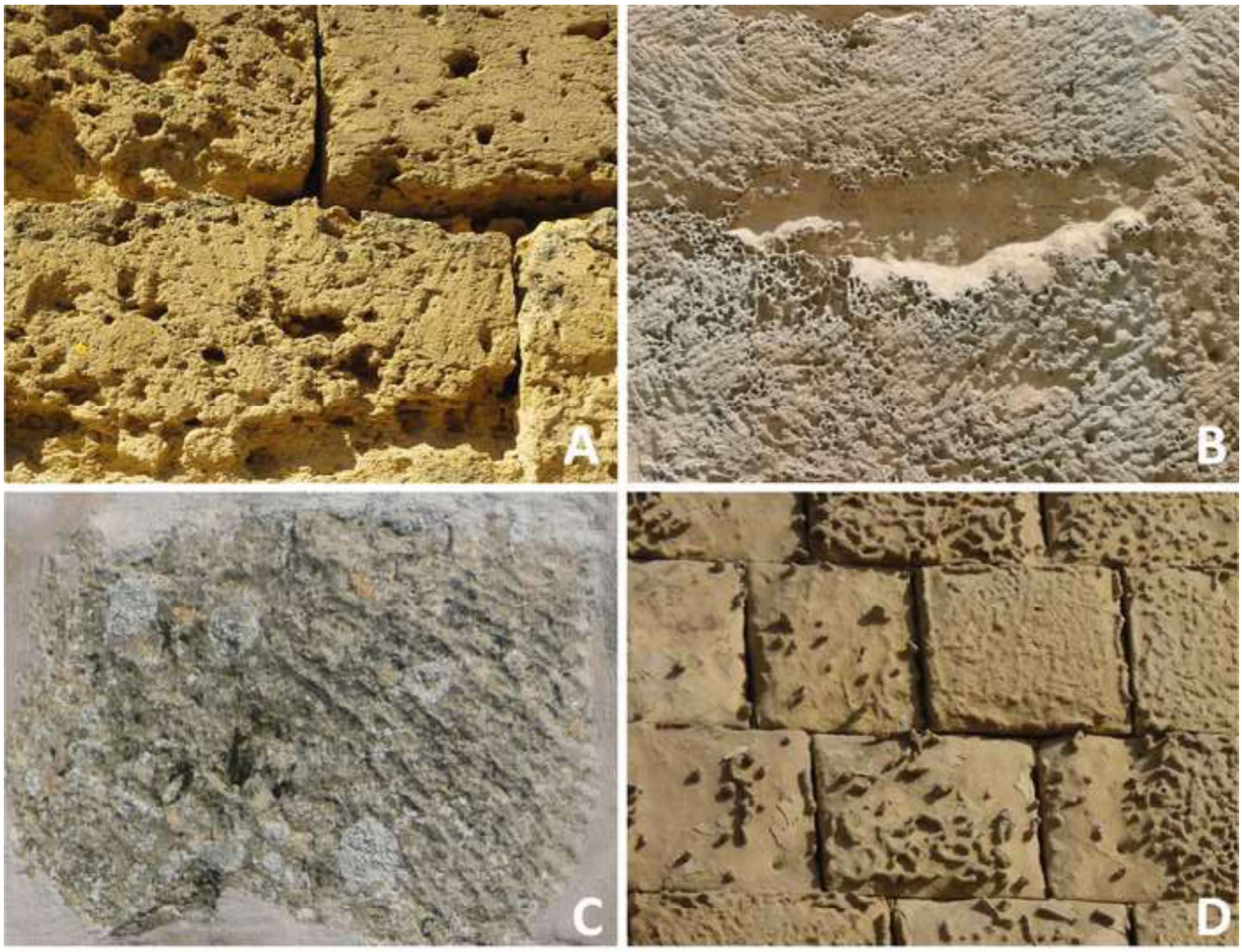

Figure 7

Click here to access/download;Figure (Color);FIG_7.JPG

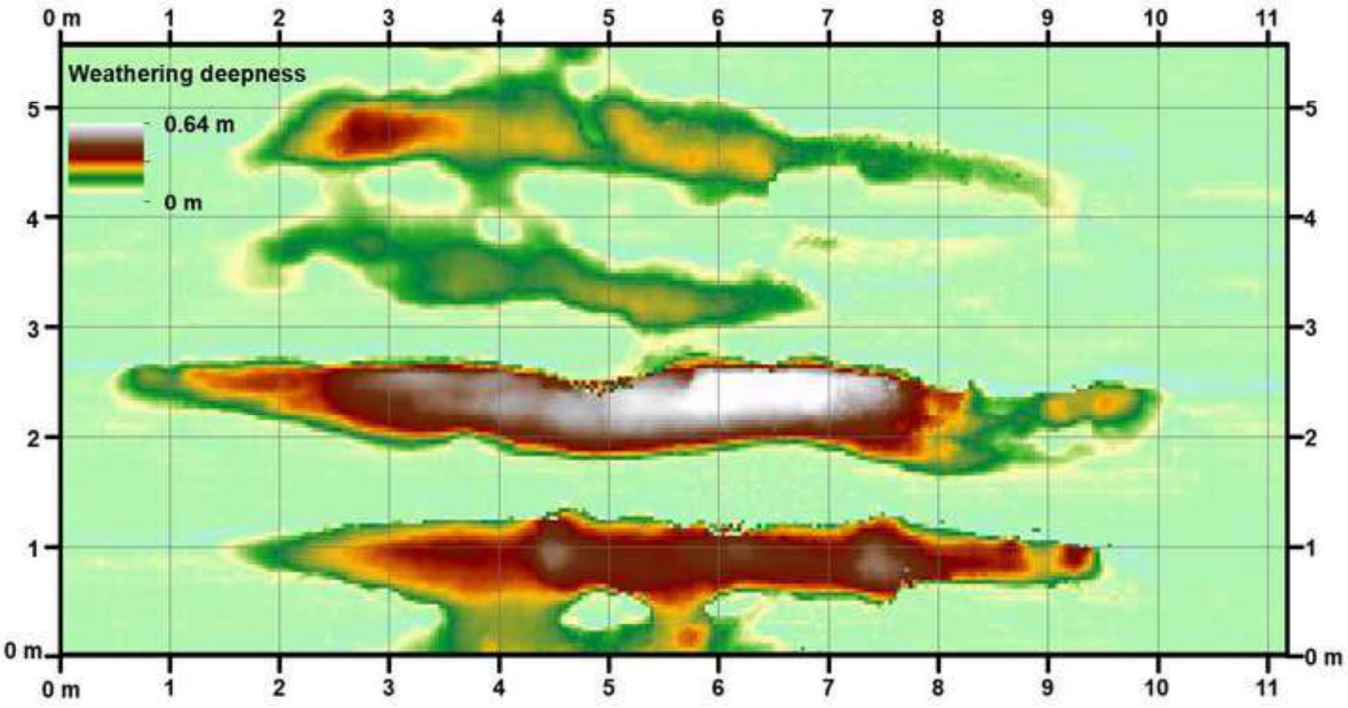

Figure 8

Click here to access/download;Figure (Color);FIG_8.jpg

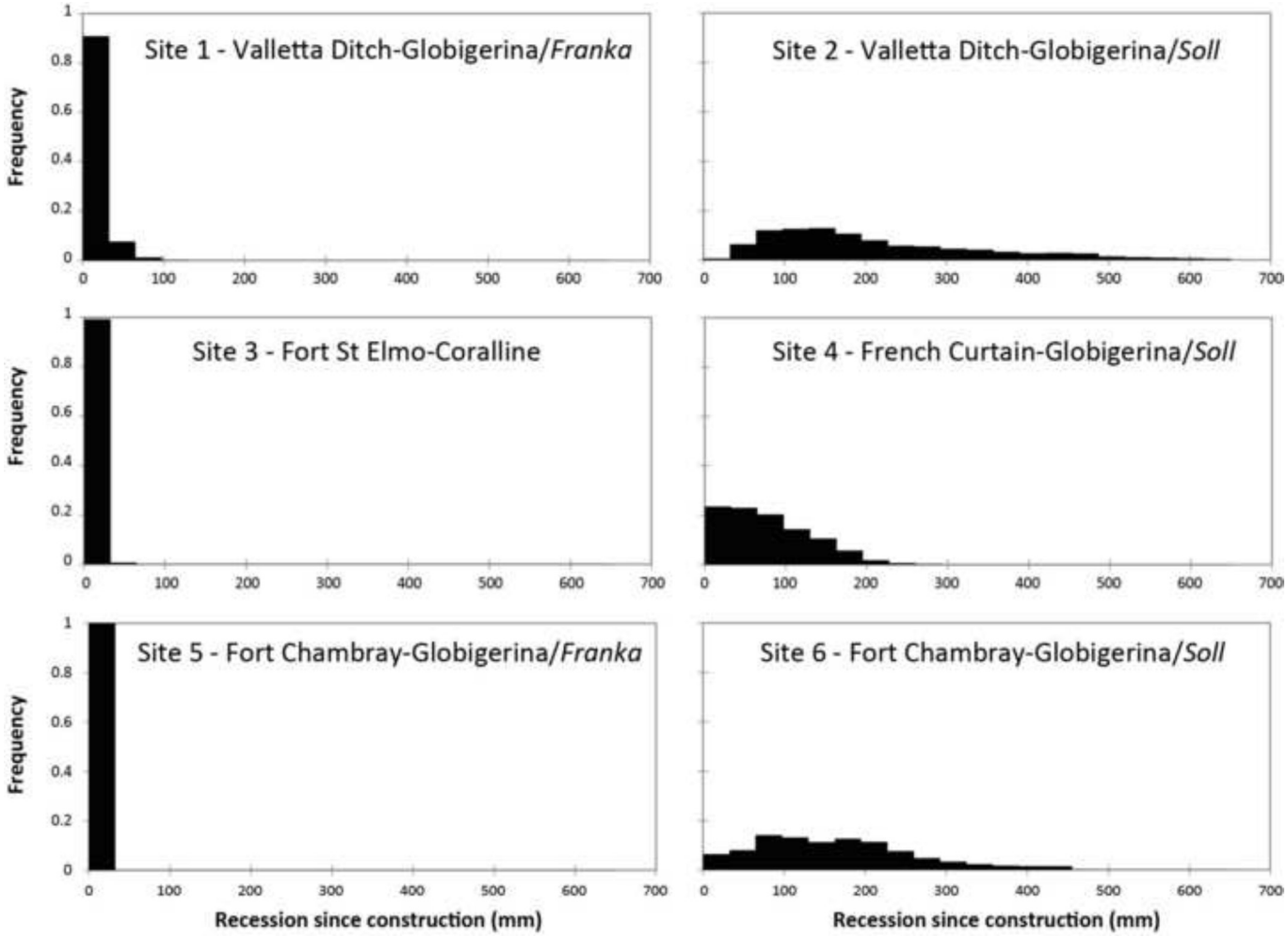

Figure 9

Click here to access/download;Figure (Color);FIG_9.jpg

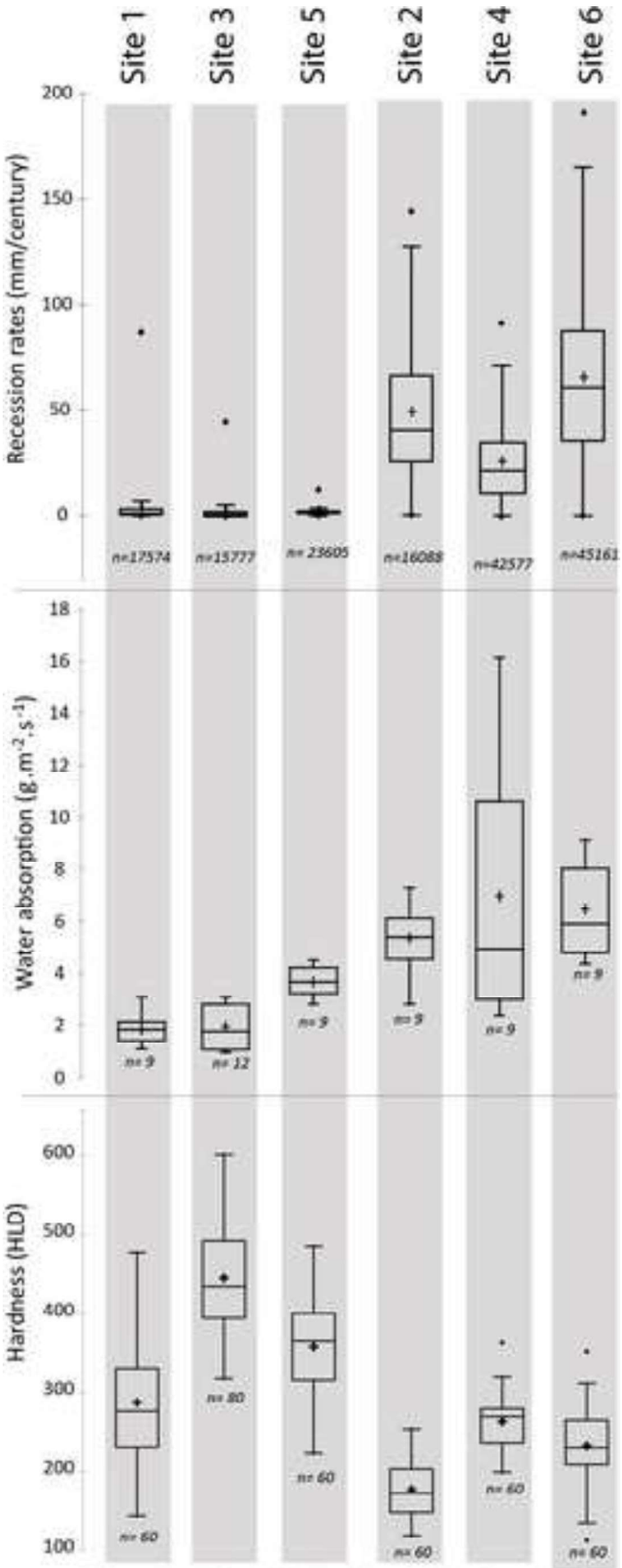

Site 1 - Valletta Ditch-Globigerina/*Franka* ; Site 2 - Valletta Ditch-Globigerina/*Soil* ; Site 3 - Fort St Elmo -Coralline ; Site 4 - French Curtain-Globigerina/*Soil* ; Site 5 - Fort Chambray-Globigerina/*Franka* ; Site 6 - Fort Chambray-Globigerina/*Soil*

Figure 10

Click here to access/download;Figure (Color);FIG_10.jpg

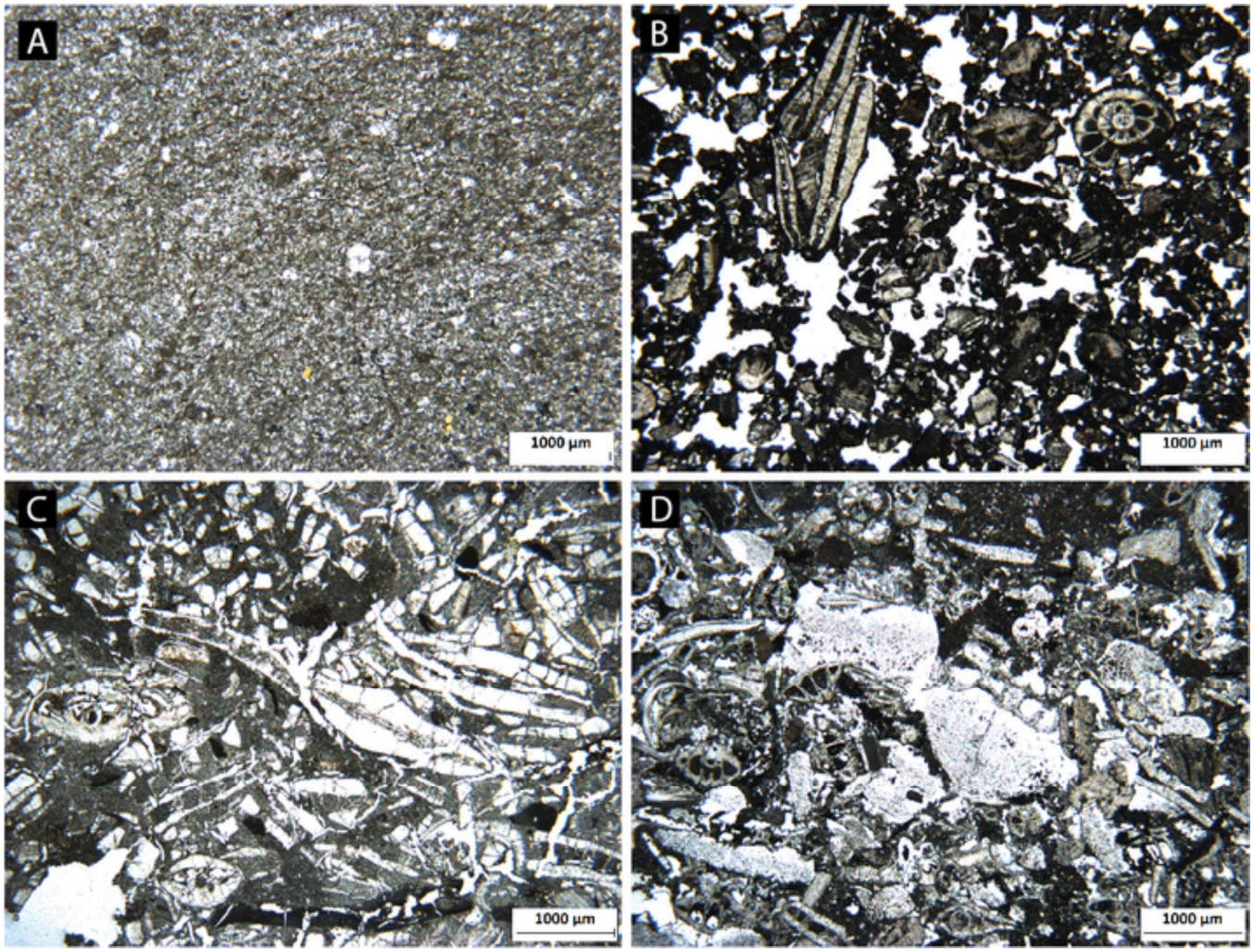

Figure 11

Click here to access/download;Figure (Color);Figure_11_resubmission.jpg

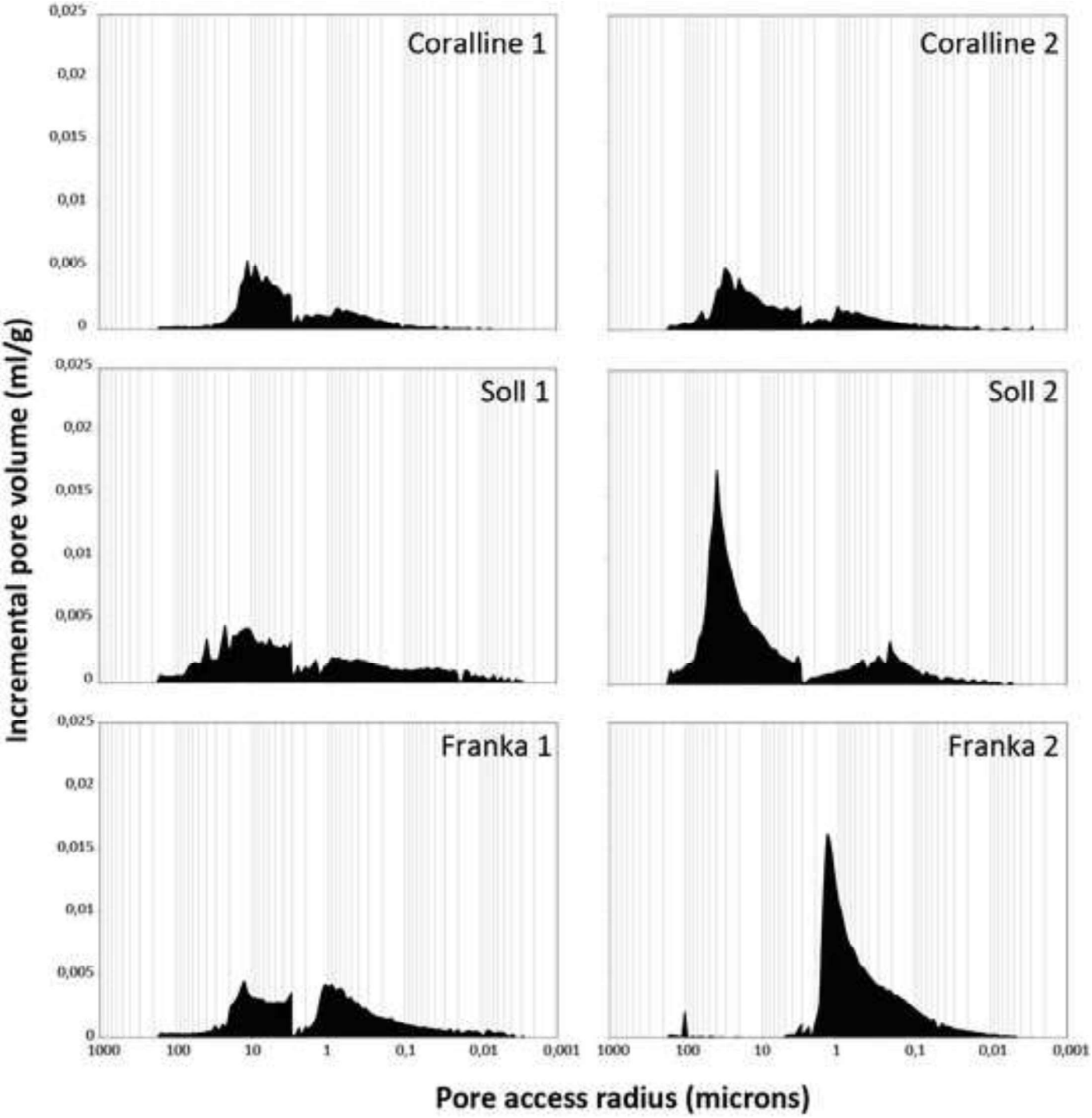

Figure 12

Click here to access/download;Figure (Color);FIG_12.jpg